A Model for HAZ Hardness Profiles in Al-Li-X Alloys: Application to the Al-Li-Cu Alloy 2095

A study was conducted to prove an earlier theoretical model and understand hardness profiles in the HAZ of Al-Li-X type alloys

BY G. O. RADING, M. SHAMSUZZOHA AND J. T. BERRY

ABSTRACT. In a previous paper (Ref. 1), details were presented of a theoretical model describing the evolution of the hardness profiles in the heat-affected zones (HAZ) of Al-Li-X weldments. The intent of the model was to qualitatively predict the general shape of such a profile, which indicates points of double inflection. In the present paper, experimental results are presented to validate the model. Panels of Al-Li-Cu Alloy 2095 in the peak aged (T8) condition were welded by the gas tungsten arc (GTA) process using AA 2319 filler metal. Conventional transmission electron microscopy (TEM) studies were conducted on specimens taken from specific points across the HAZ to estimate the relative ratios of T_1 (Al_2CuLi) and _δ′ (Al_3Li) precipitates, as well as incoherent grain boundary phases. Electron probe microanalysis (EPMA) was used to determine the variation of concentrations of elements across the HAZ, while the hardness profile was determined using Vickers microhardness measurements. The hardness profile and the associated pattern of phases present agree well with the information predicted qualitatively by the previously described model.

Introduction

Al-Li-Cu Alloy 2095 is a promising candidate for the cryogenic fuel tanks of the next generation spacecraft (Ref. 2). This derives principally from its weldability combined with its ability to reach ultra-high strengths in the peak aged (T8 or T6) temper conditions. The principal strengthening precipitate in the T8 temper condition is T_1 (Al_2CuLi) (Ref. 3). This precipitate occurs as platelets on $\{111\}_{Al}$ planes (Ref. 4). In the naturally aged (T3 or T4) temper conditions, precipitation strengthening is provided mainly by δ′ (Al_3Li) (Ref. 3). Previous work has shown that δ′ can form in this alloy system without formal solution heat treatment and quenching (Refs. 2, 5). Furthermore, the filler metal (AA 2319) that produces the most sound welds in the alloy does not contain any lithium.

Though the alloy shows good weldability, the weldment is severely undermatched. Indeed, the weldment strength is only about one-third of the T8 base metal strength (Refs. 6, 7). Moreover, hardness profiles in the HAZ of such weldments show points of double inflection similar to those of other Al-Li-X alloys, as discussed in Ref. 1. It is therefore proposed that the double inflection that occurs in Al-Li-Cu Alloy 2095 weldments are due to the concomitant effects of reversion and coarsening of T_1, precipitation of δ′ due to natural aging and diffusion of lithium and other alloying elements (which are deficient in the filler alloy) from the base metal (BM) into the weld pool. This hypothesis is tested below by direct experimentation using transmission electron microscopy (TEM) to determine the relative amounts of T_1 and δ′ at critical points across the HAZ, by Vickers hardness testing and by determining the distribution of the elements across the HAZ using electron probe microanalysis (EPMA).

KEY WORDS

Al-Li-Cu Alloy 2095
AA 2319 Filler Metal
Heat-Affected Zone
GTAW
Base Metal
Inflection
Weld Interface

Experimental

The material used in the study is one version of Al-Li-Cu Alloy 2095, heat treated to the T8 temper condition. Reynolds Metals supplied the material in the form of ¼-in. (9.5-mm) thick rolled plates. Test panels were prepared from these by butt joint welding two plates, 150 x 610 mm, parallel to the rolling direction. The variable polarity gas tungsten arc welding (GTAW) process and AA 2319 filler metal were used. The chemical composition of the BM (as determined by the supplier) and the nominal composition of the filler metal are given in Table 1.

The other welding variables were current, 150 A; voltage, 10 VAC; and welding speed, 14 in./min (5.9 mm/s).

Specimens for the hardness survey and microprobe analysis were prepared from the welded panels by cutting perpendicular to the weld direction. The specimens were ground and polished by conventional techniques using SiC paper and Al_2O_3 slurry. Hardness specimens were then etched using Keller's reagent to reveal the weld interface. TEM specimens were prepared by machining cylindrical pieces with their axes parallel to the weld bead and centered at the weld interface; at distances 2, 5 and 10 mm from the weld interface; and in the unaffected base metal. Figure 1 shows the positions from which the TEM specimens were extracted. Discs 0.5 mm thick were cut from the cylindrical pieces using a

G. O. RADING is with the Dept. of Engineering Science and Mechanics, M. SHAMSUZZOHA is with the School of Mines and Energy Development and J. T. BERRY is with the Dept. of Metallurgical and Materials Engineering, University of Alabama, Tuscaloosa, Ala.

Table 1 — Chemical Compositions of the Material Tested and the Filler Alloy (wt-%)

Alloy	Cu	Li	Mg	Ag	Ti	V	Zr	Al
2095	4.3	1.29	0.34	0.36	—	—	0.14	bal.
2319	6.3	—	—	—	0.06	0.1	0.18	bal.

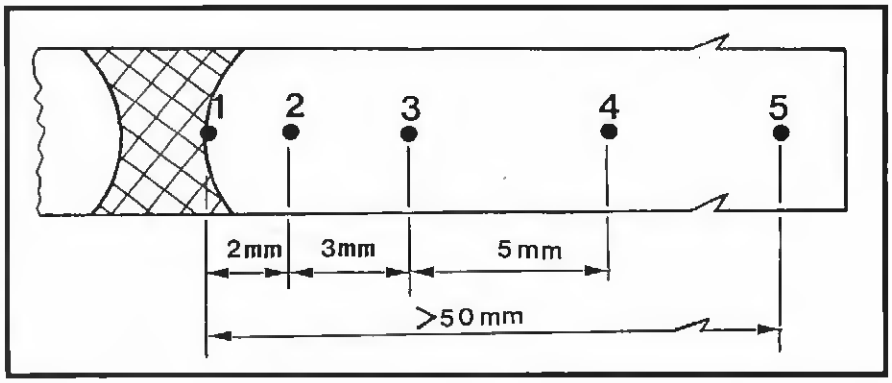

Fig. 1 — Positions from which TEM specimens were extracted.

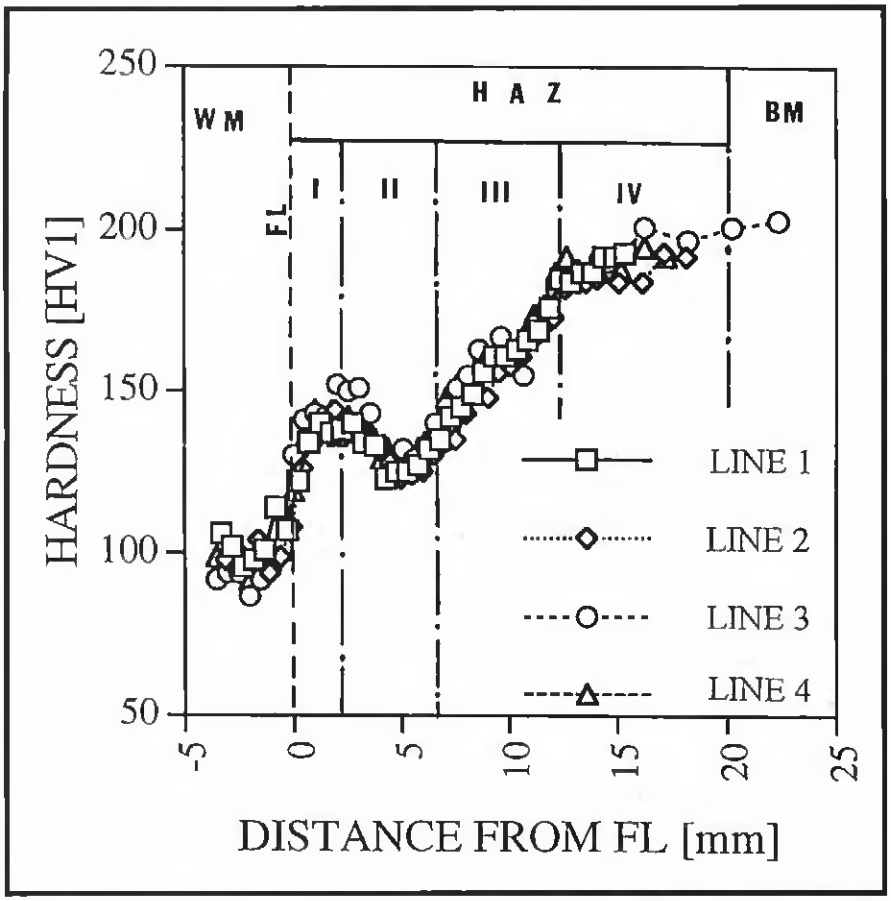

Fig. 2 — Hardness profiles across the weldment showing the four regions of the HAZ. I — fully reverted region; II — partially aged region; III — overaged region; and IV — partially reverted region.

low-speed diamond saw. The discs were then reduced to about 0.18 mm by mechanical grinding with diamond paste. Final thinning was done by twin jet electropolishing in a 30% nitric acid/methanol mixture at –25°C and 14 V. Finally, the specimens were cleaned in acetone and alcohol.

The EPMA was performed on a JOEL JXA 8600 microprobe analyzer operating at 15 kV. A Tracor Northern wavelength-dispersive X-ray spectrometer (WDS) was used for elemental analysis. Other operating conditions were a nominal beam current of 20 nA and a 40-deg beam take-off angle. The standard element table was constructed using pure elements (excluding lithium). Tests were conducted by taking scans across the weldment from the weld metal to the unaffected BM, while taking readings at intervals varying between 0.51 mm (coarse scans) and 0.06 mm (fine scans). TEM analysis was performed on a Hitachi 8000 200-kV TEM operating at 200 kV. Operating conditions included centered dark field (CDF) and bright field (BF) imaging as well as selected area diffraction (SAD). The specimens were observed mainly along the <100>, <110> and <112> zone axes of the matrix.

Results and Discussion

Hardness Survey

A number of hardness profiles across the weldment, as it approached the fully naturally aged condition, are shown in Fig. 2. These values are representative of the hardness of various specimens and across different sections of the T-S cross section. A reproducible pattern is indicated: the hardness rises from the weld interface to a maximum of about 2 mm from the weld interface. This is followed by a drop in the hardness to a minimum about 4 to 6 mm from the weld interface. The hardness then rises monotonically to the BM hardness. The four regions of the HAZ suggested in Ref. 1 are clearly revealed. The boundary between the overaged region (III) and the partially reverted region (IV) is marked by a distinct change in the slope of the curve. Comparison of Fig. 2 with the predicted profile of Fig. 2 in the previous paper (Ref. 1) reveals remarkable similarity.

Microstructural Evolution

The variation of the size and relative volume fractions of T_1 precipitates with distance from the weld interface is clearly shown by the TEM micrographs in Fig. 3A–E, which were taken along the <110> and <112> zone axes. In the unaffected base metal (Fig. 3A), the microstructure shows a dense precipitation of fine T_1 precipitates. High-resolution electron microscopy results reported elsewhere (Refs. 8, 9) revealed the precipitates to be one unit cell thick (about

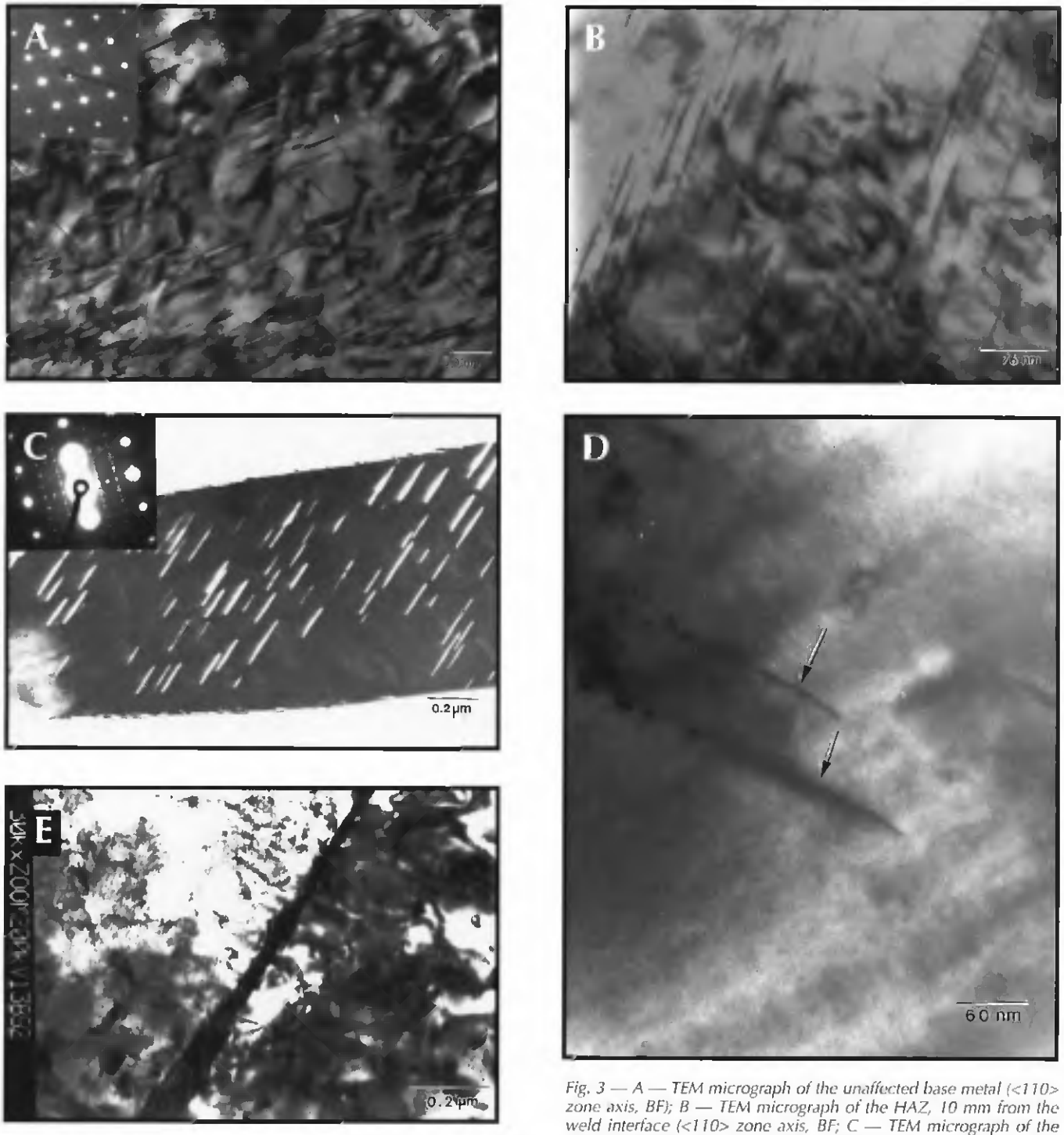

Fig. 3 — A — TEM micrograph of the unaffected base metal (<110> zone axis, BF); B — TEM micrograph of the HAZ, 10 mm from the weld interface (<110> zone axis, BF; C — TEM micrograph of the HAZ, 5 mm from the weld interface (<112> zone axis, CDF using T_1 {1101} reflection); D — microstructure of the HAZ, 2 mm from the weld interface showing a few partially dissolved T_1 precipitates (arrowed); E — microstructure at the weld interface showing no T_1 precipitation (<110> zone axis, BF).

1 nm). Their diameter can be used for comparison purposes only, since the viewing plane does not transect all of them through their center. At the 10-mm distance (Fig. 3B), considerable precipitation of T_1 is still evident. However, the precipitates have grown somewhat, indicating coarsening at this point.

The microstructure 5 mm from the weld interface is shown in Fig. 3C. Compared to the BM (Fig. 3A), considerable coarsening is seen to have taken place. At the 2-mm distance (Fig. 3D), most of the T_1 precipitates have dissolved. However, a few partially dissolved T_1 precipitates are visible, but these clearly cannot contribute anything to the strengthening. At the weld interface (Fig. 3E), no T_1 precipitates are visible in the microstructure. However, evidence of the presence of _δ′ can be seen from the superlattice spots in the diffraction pattern.

The variation of _δ′ and _θ′ with distance from the weld interface is shown in Fig. 4A–E. At the BM (Fig. 4A), there is virtually no _δ′ and only sparsely distributed _θ′. At the 10-mm distance, the amount of _δ′ has increased somewhat, but its possible contribution to hardening is clearly negligible. At the 5-mm

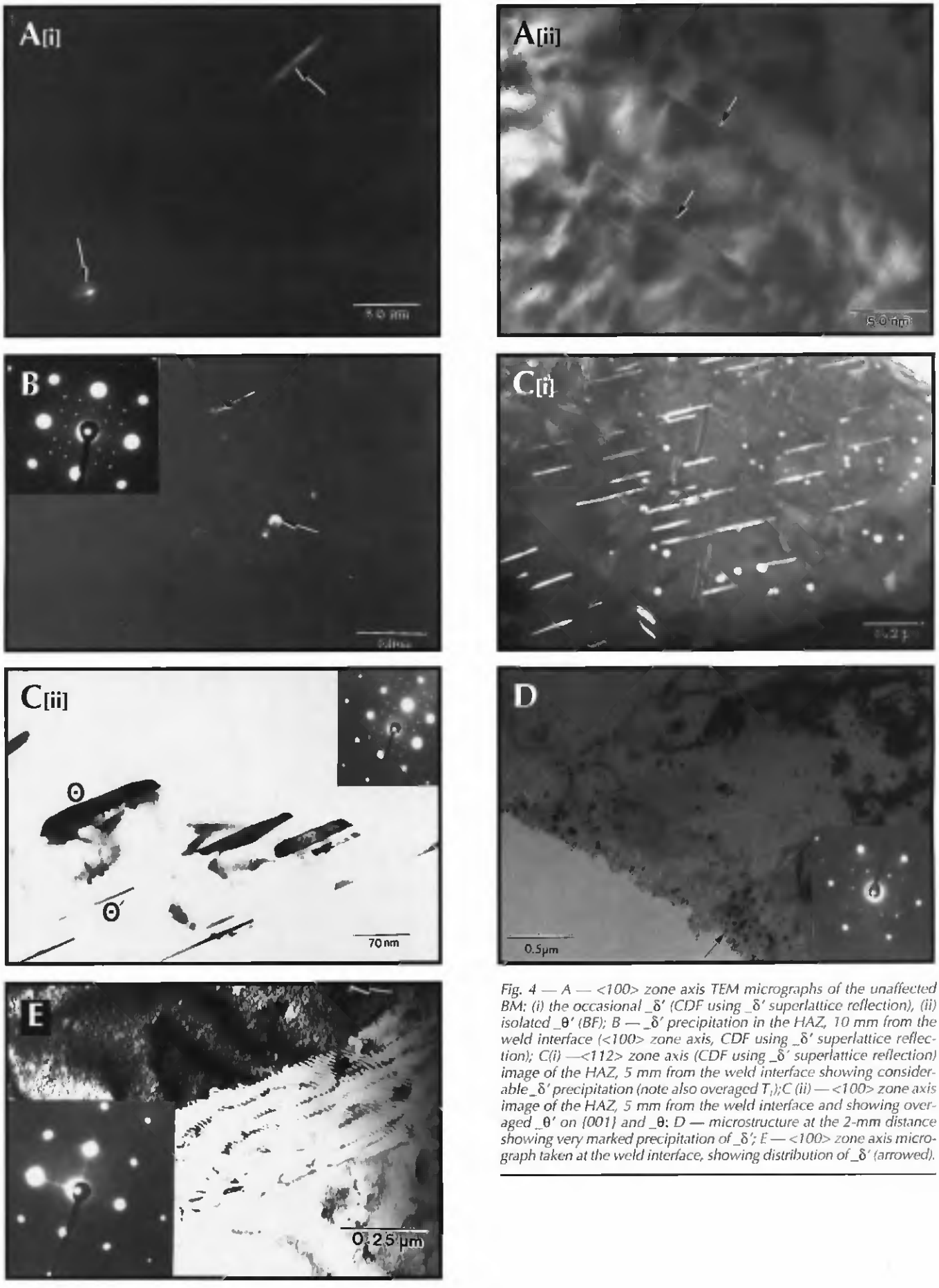

Fig. 4 — A — <100> zone axis TEM micrographs of the unaffected BM: (i) the occasional _δ′ (CDF using _δ′ superlattice reflection), (ii) isolated _θ′ (BF); B — _δ′ precipitation in the HAZ, 10 mm from the weld interface (<100> zone axis, CDF using _δ′ superlattice reflection); C(i) —<112> zone axis (CDF using _δ′ superlattice reflection) image of the HAZ, 5 mm from the weld interface showing considerable _δ′ precipitation (note also overaged T1);C (ii) — <100> zone axis image of the HAZ, 5 mm from the weld interface and showing overaged _θ′ on {001} and _θ; D — microstructure at the 2-mm distance showing very marked precipitation of _δ′; E — <100> zone axis micrograph taken at the weld interface, showing distribution of _δ′ (arrowed).

Fig. 5 — A TEM micrograph showing an example of incoherent grain boundary precipitation in the HAZ 2 mm from the weld interface.

interface is shown in Fig. 4E. The figure shows no _θ′ at this point and the amount of _δ′ is much less than at the 2-mm point. In addition to the above microstructural changes, copious precipitation of grain boundary phases was noted to various extents throughout the HAZ. An example is shown in Fig. 5.

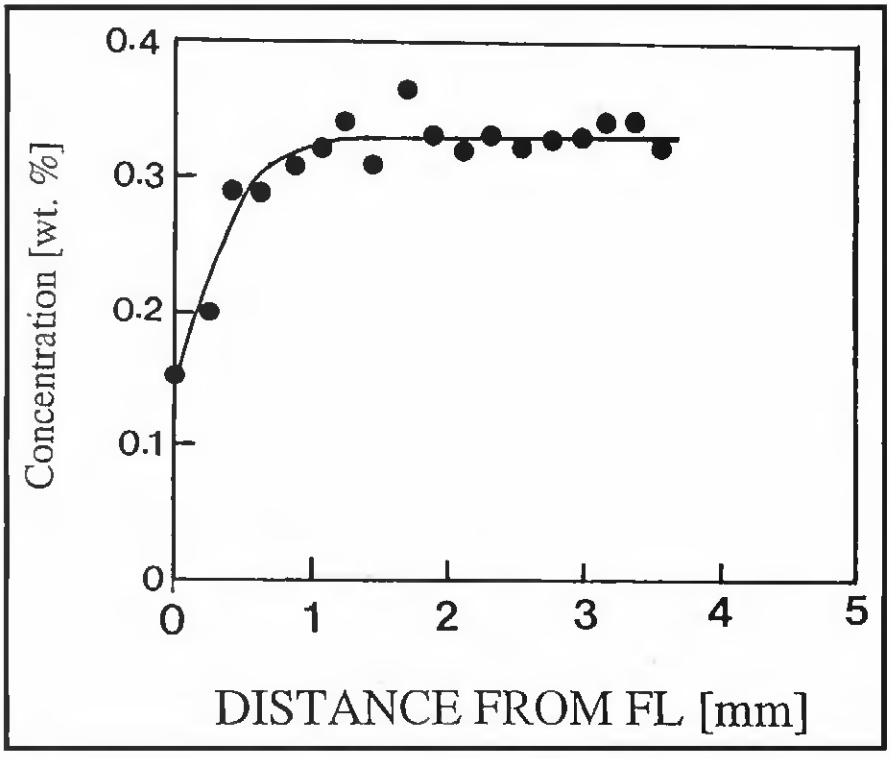

Fig. 6 — Variation of magnesium content across the HAZ.

distance, considerable quantities of _δ′ and _θ′ are evident. Comparison with Fig. 4A(ii) reveals that considerable coarsening of _θ′ has taken place at the 5-mm distance, similar to the effect on T_1. At the 2-mm distance, however, a very marked precipitation of _δ′ can he noted — Fig. 4D. Moreover, the precipitates have grown to a considerable size (about 50 nm), such that the Orowan looping mechanism of strengthening is likely to be operative. It is this strengthening from _δ′ that produces the maximum at the 2-mm distance in the hardness profile. The <100> zone axis micrograph of the weld

Elemental Diffusion

Since lithium is undetectable by X-ray dispersive techniques, the variation of lithium content could not be determined. However, for the current study, what is important is the variation of lithium content across the HAZ that would help determine if diffusion has taken place and if the variation is roughly exponential as predicted hy Equation 19 in Ref. 1. To illustrate the nature of elemental diffusion, the variation in the concentration of magnesium (whose diffusivity in aluminum is close to that of lithium, and which, like lithium, is deficient in the filler metal) across the HAZ is shown in Fig. 6. The variation of magnesium content with distance is roughly exponential, with the lowest value at the weld interface, before leveling off to the BM concentration (0.34%). The variation of silver content (silver is also in the BM but deficient in the filler alloy) showed a similar profile. It is reasonable to assume that the lithium content follows a similar profile. The diffusion of these elements into the weld pool is therefore highly likely. The variation in the quantity of _δ′ between the weld interface and the 2-mm distance can therefore be understood in terms of lithium diffusion.

The results presented here agree with the theory presented in Ref. 1. The hardness profile shows points of douhle inflection similar to what is reported for other Al-Li-X alloys. The maximum is clearly due to the precipitation of fully developed _δ′ precipitates. This marked precipitation of _δ′ stems from its ability to form without the benefit of a formal solution treatment and quenching. Since _δ′ forms from dissolved lithium that was originally part of T_1, optimum formation occurs where dissolution of T_1 is complete and yet is far enough from the weld pool to preclude considerable diffusion of lithium into the weld pool. Other effects not considered in the theory but evident in the experimental results are the following:

1) The part played by incoherent grain boundary precipitates. To model the effect of these, it is necessary to know, or predict, their nature and crystal structure; be able to relate their size, distribution and volume fraction to the strength of the welding thermal cycle; and then develop constitutive equations relating these to their contribution to softening. To date, no such data is available in the literature and it is doubtful if the extra accuracy obtainable would be worth the extra effort. To a first approximation, therefore, their effect can be neglected.

2) The theoretical development considered only one plate-like precipitate in the base metal, while the results show considerable quantities of _θ′, especially at the 5-mm distance. A more rigorous development would require that the kinetics of all precipitates in the BM be considered.

3) Recrystallization. The thermal cycle causes changes in the grain structure in addition to the changes in submicron structure considered so far. A parallel study (Ref. 10) revealed such an effect in the current alloy. This affects the terms H_{gb} and H_t in Equation 1 in Ref. 1 (*i.e.*,

hardening due to the Hall-Petch effect and texture, respectively). Similarly, dissolution of precipitates into the matrix causes changes in the solution hardening term, H_{ss}. However, to a first approximation, these effects can be considered negligible compared to precipitation strengthening.

Summary and Conclusions

A TEM study of the microstructural evolution in the HAZ of the Al-Li-Cu Alloy 2095 was undertaken with the aim of understanding hardness profiles in the HAZs of weldments of Al-Li-X-type alloys. Reasonable agreement was obtained between the results and the theoretical model, based on reaction kinetics, developed in Ref. 1. The following are salient points of both the theory and experiment:

1) The hardness profile in the HAZ shows points of double inflection before increasing, almost monotonically, to the hardness of the BM. The effect is due to the concurrent effects of T_1 dissolution, T_1 coarsening, natural aging and diffusion of alloying elements that are deficient in the filler alloy from the HAZ into the weld pool.

2) A maximum (which in Alloy 2095 occurs 2 mm from the weld interface) corresponds to the maximum precipitation of _δ′ (Al_3Li) due to natural aging after dissolution of T_1.

3) Reduction in hardness from the position of the maximum to the weld interface occurs due to diffusion of alloying elements that are deficient in the filler alloy into the weld pool, thus reducing the propensity for _δ′ precipitation.

4) The minimum (which occurs 5 mm from the weld interface in Alloy 2095) corresponds to the point at which T_1 coarsening is most pronounced.

5) The monotonic rise in hardness from the minimum to the BM corresponds to increasingly less dissolution/ coarsening of T_1 as the peak temperature attained in the weld thermal cycle decreases.

Acknowledgments

We are grateful to Dr. Carl Cross of Martin Marietta, whose company supplied the material and carried out the welding for this study. This research utilized facilities of the School of Mines and Energy Development at the University of Alabama. We wish to acknowledge the assistance of Dr. Michael Bersch with the EPMA. G. O. Rading acknowledges with thanks financial support from USIA through the Fulbright program.

References

1. Rading, G. O., and Berry, J. T. 1998. A model for HAZ hardness profiles in Al-Li-X alloys. *Welding Journal* 77(9): 383-s to 387-s.

2. Pickens, J. R., Heubaum, F. H., Langan, T. J., and Kramer, L. S. 1989. *Proc. of 5th Intl. Al-Li Conf.*, eds. T. H. Sanders, Jr., and E. A. Starke, Jr., p. 1397. MCE Pub., Williamsburg, Va.

3. Langan, T. J., and Pickens, J. R. 1989. *Proc. of 5th Intl. Al-Li Conf.*, eds. T. H. Sanders, Jr., and E. A. Starke, Jr., p. 691. MCE Pub., Williamsburg, Va.

4. Huang, J. C., and Ardell, A. J. 1989. 4th Intl. Al-Li Conf., eds. G. Champier, B. Dubost, D. Miannay and L. Sabetay, p. 373. *Journal de Physique*, 48, Colloque C3.

5. Gayle, F. W., Heubaum, F. H., and Pickens, J. R. 1990. *Scripta Metall. Mater.* 24 p. 79.

6. Sunwoo, A. J., and Morris, J. W. 1991. *Mater. Sci. Technol.* 7. p. 965.

7. Cross, C. E., and Edwards, G. R. 1989. *Treatise on Materials Science and Technology*, Vol. 31, eds. A. K. Vasudevan and R. D. Doherty, p.171. Academic Press.

8. Rading, G. O., Shamsuzzoha, M., and Berry, J. T. 1994. A TEM and high resolution microstructural characterization of the Al-Li-Cu alloy 2095 in the T8 temper condition. *ACEM-13: 13th. Conf. Australian Society for Electron Microscopy*, Brisbane, Australia.

9. Easterling, K. 1992. *Introduction to the Physical Metallurgy of Welding*, Butterworth-Heinemann, Oxford, U.K.

10. Rading, G. O. 1994. Fatigue Crack Growth in Welded Al-Li-Cu Alloy 2095 (Weldalite™ 049). Ph.D. dissertation, University of Alabama.